

Poly(A) binding protein, C-terminally truncated by the hepatitis A virus proteinase 3C, inhibits viral translation

Bo Zhang¹, Graziella Morace², Verena Gauss-Müller^{1,*} and Yuri Kusov¹

¹Institute of Medical Molecular Biology, University of Lübeck, Germany and ²Istituto Superiore di Sanita, Rome, Italy

Received July 6, 2007; Revised August 2, 2007; Accepted August 3, 2007

ABSTRACT

Proteolytic cleavage of translation initiation factors is a means to interfere with mRNA circularization and to induce translation arrest during picornaviral replication or apoptosis. It was shown that the regulated cleavages of eukaryotic initiation factor (eIF) 4G and poly(A)-binding protein (PABP) by viral proteinases correlated with early and late arrest of host cap-dependent and viral internal ribosome entry site (IRES)-dependent translation, respectively. Here we show that in contrast to coxsackievirus, eIF4G is not a substrate of proteinase 3C of hepatitis A virus (HAV 3C^{pro}). However, PABP is cleaved by HAV 3C^{pro} *in vitro* and *in vivo*, separating the N-terminal RNA-binding domain (NTD) of PABP from the C-terminal protein-interaction domain. *In vitro*, NTD has a dominant negative effect on HAV IRES-dependent translation and an enhanced binding affinity to the RNA structural element pY1 in the 5' nontranslated region of the HAV RNA that is essential for viral genome replication. The results point to a regulatory role of PABP cleavage in RNA template switching of viral translation to RNA synthesis.

INTRODUCTION

Translation initiation of capped mRNA is remarkably stimulated by the 3' poly(A) tail. This synergistic effect on translation was attributed to interactions between the eukaryotic translation initiation factor (eIF) complex eIF4F and the poly(A)-binding protein (PABP) (1–5). eIF4F consists of the cap-binding protein eIF4E, the ATP-dependent RNA helicase eIF4A, and eIF4G that serves as a scaffold for the binding of several proteins, including eIF4E, eIF4A and eIF3. In addition, eIF4G

contains in its N-terminal part a binding site for PABP. The simultaneous binding of eIF4G to the cap-bound eIF4E and PABP associated with the poly(A) tail can bring the RNA ends in close proximity and circularize mRNA, thereby allowing ribosome recycling (5,6). Cytoplasmic PABP is an abundant protein of 70 kDa that has been recognized as a true translation initiation factor (7–9). It contains four RNA recognition motifs (RRM) in its N-terminal domain (NTD) that are involved in RNA and eIF4G binding (10). A proline- and glutamine-rich linker region connects the NTD to the C-terminal domain (CTD) that interacts with various proteins involved in both translation initiation (eIF4B, 60S ribosomal subunit) as well as termination (releasing factor eRF3). In addition, the CTD mediates PABP oligomerization that contributes to the cooperative binding to poly(A) sequences longer than 12 residues. Besides its function in translation, PABP controls mRNA stability and plays additional roles in the regulation of gene expression (11,12).

Picornaviruses have a messenger-sense RNA genome of ~7500 bases, with a large open reading frame that is flanked by 5' and 3' nontranslated regions (NTR) and terminated by a poly(A) tail of more than 60 residues. In place of the cap structure, the 5' end of the viral genome is covalently attached to the small protein VPg that is the primer of RNA synthesis. Replication of most picornaviruses in cell culture is associated with cytopathology. These viruses have evolved various mechanisms to ensure efficient viral translation, often at the expense of host protein synthesis. Viral proteins rearrange cell membranes and viral proteinases impact the structure and localization of host cell proteins. Among the identified cellular targets, eIF4G is cleaved by poliovirus (PV) proteinase 2A or foot-and-mouth-disease virus proteinase Lb, resulting in the abrogation of cap-dependent translation of host mRNAs early in infection (13–15). PABP cleavage by coxsackievirus B3 (CVB3) or PV proteinases 2A^{pro} and 3C^{pro} seems to occur later in the viral life cycle (16–19). Overall,

*To whom correspondence should be addressed. Tel: +49 451 500 4085; Fax: +49 451 500 3637; Email: gaussmue@molbio.uni-luebeck.de
Present address:

Bo Zhang, DAI 4085, Wadsworth Center, New York State Department of Health, 120 New Scotland Ave, Albany, New York, 12208, USA.

these studies demonstrated that cytolitic picornaviruses down-regulate host metabolism mostly by drastically inhibiting cellular translation, while viral translation continues via a cap-independent mechanism.

As a member of the hepatovirus genus, the hepatitis A virus (HAV) is genetically and phenotypically distinct from the other members of the picornavirus family (e.g. enterovirus, rhinovirus, coronavirus and aphthovirus). Whereas most other picornaviruses contain—besides the major proteinase 3C—a second proteolytic activity in their polyprotein, which is predominantly causing host shut-off, the HAV polyprotein lacks such an activity. The HAV 5'NTR of 734 residues comprises *cis*-acting elements involved in genome replication and translation initiation. Computer-assisted folding predictions and biochemical probing showed that the HAV 5'NTR forms extensive higher order structures which include six stem-loop domains [(20–25), see Figure 5 for a simplified outline of essential parts of the HAV 5' NTR]. The 5' most terminal domain (bases 1 to 95) contains a hairpin and two pseudoknots and is followed by a pyrimidine-rich tract (pY1, bases 96 to 148). These parts of the 5'NTR are involved in viral replication (26). The remainder of the 5'NTR (bases 155 to 734) functions as an internal ribosome entry site (IRES), allowing cap-independent translation initiation. Owing to its unique structure and due to diverse requirements for optimal activity, the HAV IRES (type III IRES) substantially differs from the IRES of other picornaviruses and that of the hepatitis C virus (20,21,27,28). The HAV IRES interacts with a number of host proteins, such as the poly(rC)-binding protein 2 (PCBP2) (29), glyceraldehyde-3-phosphate dehydrogenase (GAPDH) (30,31), the polypyrimidine tract-binding protein [PTB; (31,32)] and eIF4GI (27,33). The role of these interactions is still elusive. Following uptake of the viral messenger-sense RNA into the cell, the viral polyprotein is synthesized through internally initiated translation at the IRES. The HAV proteinase 3C^{pro}, that itself is a part of the polyprotein, catalyzes the subsequent liberation of the structural and nonstructural proteins. Together with host proteins, the latter assemble into the viral replication complex and viral RNA synthesis starts with the generation of a negative strand intermediate. As translation and negative strand synthesis are competing processes that proceed in opposite directions on the infecting viral genome, the translating viral RNA must be cleared of initiating or recycling ribosomes before RNA synthesis can begin (34). In this context, the observation is interesting that polioviral genomes that have not been translated cannot function as template for RNA synthesis. The molecular mechanisms regulating this selection of viral RNA template functions are currently scrutinized.

Most strikingly and in sharp contrast to the cytolitic picornaviruses, replication of most HAV strains is highly protracted and noncytotoxic in cell culture. One way to ensure viral persistence in culture is the observed suppression of cellular antiviral defense mechanism by HAV (35). As no effect on the host metabolism has been detected so far in HAV-infected cells, it appears that HAV remains in a state of constant competition with host translation and never reaches a privileged stage of protein

synthesis (1,36,37). Beyond competing with host protein synthesis, production of the HAV polyprotein clearly conflicts with HAV RNA synthesis at later phases of the viral life cycle. In particular, it is not clear how HAV translation is stalled to allow RNA synthesis to occur. It is tempting to speculate that once enough of the replication complex is formed, one or several of its components interfere with HAV translation initiation by affecting essential translation factor(s). Here, we present evidence that—unlike the enteroviruses—HAV proteinase 3C^{pro} does not cleave eIF4G. However, HAV 3C^{pro} cleaves PABP *in vitro* and *in vivo* and exploits its cleavage product. We show that the NTD of PABP has improved RNA-binding capacity to the pY1 in the HAV 5'NTR and specifically suppresses HAV IRES translation pointing to its regulatory function in halting viral protein synthesis.

MATERIALS AND METHODS

Plasmids and *in vitro* transcription

Plasmids pET15b-3ABCwt, pET15b-3ABCm and pET15b-3ABC μ that encode various precursor forms of HAV 3C were described before (38). pET28-hPABP (kindly provided by M. Görlach) encodes the complete PABP with an N-terminal His-tag (9). pET28-PABP1234 (kindly provided by G.J. Goodall) encodes the N-terminal domain (NTD) of PABP with four RNA-binding motifs and a N-terminal His-tag (39). pET28-PABP-CT [kindly provided by M. Kiledjian; (40)] encodes the His-tagged CTD. The HAV replicon (pT7-18f-Luc-A60) was described before (41). The poliovirus replicon pRluc31 was kindly provided by R. Andino (42). Luciferase-encoding replicon RNA was prepared according to the user manual of the T7 RiboMAX Large Scale RNA production system (Promega), after linearization of the HAV replicon cDNA with AgeI and the PV replicon with MluI. pHAV-IRES-luc encodes the firefly luciferase that is preceded by the HAV IRES (HAV nucleotides 44–736) (3). pHAV-IRES-luc was linearized with NotI prior to *in vitro* transcription with T3 RNA polymerase. Radiolabeled RNAs was prepared as described in the manual of the MaxiScriptTM *in vitro* transcription kit (Ambion), with 3 μ l α -[³²P]-UTP (10 μ Ci/ μ l) and additional 2 μ l UTP (0.05 mM) in a 20 μ l volume. To generate 3' NTR-A20 and 3'NTR-A60 transcripts, pT7-18f-(Δ P1-P3)-A20 and pT7-18f-(Δ P1-P3)-A60 were linearized with AgeI and used as template for T7 transcription (43). pT7-18f-(Δ P1-P3) A0rbz was linearized with RsrII to generate the 3' NTR-A0 transcript. To produce RNA1-94 and RNA95-148, pGEM1-HM175-1-95 and pGEM1-HM175-95-736 were linearized with EcoRI or SspI, respectively, and transcribed with SP6 RNA polymerase (44). Radiolabeled RNA was purified, and dissolved in 50 μ l RNase-free water.

Recombinant proteins

Plasmids pET28-hPABP, pET28-PABP1234 and pET28-PABP-CT were expressed in *Escherichia coli* strain BL21 (DE3) pLysS as described (39,40,45). The soluble proteins were purified using HisTrap chelating HP columns as

recommended by the manufacturer (Amersham Biosciences, USA). The eluted proteins were concentrated and transferred into 50 mM Tris-HCl, pH 8.0, 50 mM NaCl, 15% glycerol using a centrifugal filter device (Amicon Ultra 30 000). Purified 3C of HAV and coxsackievirus B3 (CVB3; kind gift of R. Zell) were described previously (45,46).

RNA-protein interaction determined by electrophoretic mobility shift assay (EMSA)

EMSA was essentially performed as described before (44,47,48). [³²P]-labeled riboprobes (2.5×10^5 c.p.m.) were incubated with increasing amounts of purified PABP or NTD (50–700 nM) in 15 μ l reaction buffer containing 5 mM HEPES, (N-2-hydroxyethylpiperazine-N'-ethansulfonic acid), pH 7.9, 25 mM KCl, 2 mM MgCl₂, 1.75 mM ATP, 6 mM dithiothreitol (DTT), 0.05 mM phenylmethylsulfonyl fluoride, 166 μ g/ml of *E. coli* tRNA, and 5% glycerol. After 20 min at 30°C, the mixture was supplemented with 5 μ l of sample buffer (1 mM EDTA, 0.25% bromophenol blue (BPB), 0.25% xylene cyanol, 50% glycerol) and analyzed by electrophoresis using a 6% nondenaturing polyacrylamide gel (PAGE). Electrophoresis was conducted in 0.5 \times Tris-borate buffer at 150 V for 30–90 min until the BPB marker had migrated to 2/3 of the gel length. The gel was scanned using a PhosphorImager (Fujifilm BAS 1000, Japan) and the image was analyzed with the analysis software PCBAS (Raytest, Isotopemessgeräte GmbH, Germany). The apparent equilibrium-binding constant (app. K_{eq}) was calculated according to Lane *et al.* (49).

Proteolytic cleavage *in vitro*

Four-hundred nanogram-purified recombinant PABP and various amounts of HAV or CVB3 proteinases 3C^{Pro} (final concentration, 1–10 μ M) were incubated at 37°C for 6–24 h in cleavage buffer (19). The reaction was stopped by the addition of sodium dodecylsulfate (SDS)-PAGE sample buffer and the products were analyzed by SDS-PAGE, followed by immunoblot with anti-3C, anti-PABP or anti-His. For cleavage of PABP and eIF4G in cell fractions (S10, S200 and P200, see subsequently), 10 μ l of the extracts were incubated with HAV 3C^{Pro} (7 μ M final concentration). The cleavage products were detected by immunoblot using anti-eIF4G or anti-PABP.

Viruses and cells

HAV strain 18f was propagated in the human hepatoma cell line Huh-7. For HAV infection, cells were inoculated for 3 h at 37°C with the soluble extract of HAV-infected cells at a multiplicity of infection (moi) of 1 tissue culture infectious dose₅₀/cell in OptiMEM (Invitrogen). Infected cells were incubated in Dulbecco's-modified Eagle medium (DMEM) with 2% fetal calf serum for the indicated time periods. The recombinant vaccinia virus vTF7-3 that encodes T7 RNA polymerase was amplified in COS-7 cells and the virus stock was plaque titrated by serial 10-fold dilutions (50). The working dose of vTF7-3 as a helper virus to aid the expression of T7-promoted genes was characterized by quantification of luciferase

activity after transfection of pT7-LUC (Luciferase T7 Control DNA, Promega), followed by infection with vTF7-3.

Proteolytic cleavage *in vivo*

For coexpression, Huh-T7 cells that constitutively express T7 RNA polymerase were used (25). They were grown in DMEM in the presence of geneticin (G-418 sulfate, 400 μ g/ml), penicillin (100 U/ml) and streptomycin sulfate (100 μ g/ml). pET28-hPABP and plasmids encoding HAV 3C^{Pro} were cotransfected into 5×10^5 cells. The transfection mixture containing 1 μ g cDNA and 8 μ l Lipofectamin (Invitrogen) in 200 μ l OptiMEM was pre-incubated for 30 min at room temperature and diluted with OptiMEM to 1 ml before applying to 80% confluent cells. After incubation for 3 h at 37°C, transfected cells were infected with vTF7-3 (moi \sim 1). After 1 h at 37°C, the inoculum was replaced with DMEM containing 10% fetal calf serum and antibiotics. After incubation for 24–48 h at 37°C, the cells were scraped in 250 μ l phosphate-buffered saline containing 0.05% Tween-20 and lysed by three cycles of freeze/thawing. The clarified supernatant was used for reporter gene detection and/or for immunoblot analyzes with anti-PABP or anti-His-tag. To confirm the expression of viral proteinase 3C^{Pro}, the transferred proteins were also tested with anti-HAV 3C^{Pro} raised against the recombinant proteinase (46). To determine PABP cleavage in the course of the HAV infection, extracts of infected cells were obtained as described above and analyzed by immunoblot with anti-PABP.

Immunological assays

After electrophoretic separation by SDS-PAGE (10 or 12% polyacrylamide) and transfer onto a nitrocellulose membrane (Protran, Schleicher & Schuell, Bioscience), the blots were probed either with monoclonal anti-His (Novagen), anti-PABP or anti-eIF4G1 directed against the peptide KKEAVGDLLDAFKEVN representing amino acid residues 523–538 of the N-terminus [(51); kind gift of R.E. Rhoads]. Anti-PABP was raised against a synthetic peptide sequence (GIDDERLRKEFSPFGTC) in the RRM4 of human PABP (kind gift of R. Lloyd). The particle-specific enzyme-linked immunosorbent assay (ELISA) with the monoclonal anti-HAV 7E7 (Mediagnost, Germany) and its horseradish peroxidase conjugate were applied to detect viral particles as described (52,53).

Preparation of cell extracts and *in vitro* translation

Cell extracts were prepared as described elsewhere (34,54). In brief, Huh-7 cells at 90% confluence were suspended and harvested by centrifugation (800g, 4°C, 6 min). After washing with PBS, the cell pellet was re-suspended in 2 vol of hypotonic buffer (50 mM KCl, 25 mM HEPES, 1.6 mM MgCl₂, 1 mM DTT). The suspension was allowed to swell on ice for 15 min, before lysing with 15 strokes of a Wheaton Douncer. Then 1/9 vol of 10 \times concentrated HNG buffer (25 mM HEPES, pH 7.5, 1 M potassium acetate, 30 mM MgCl₂, 30 mM DTT) was added. The debris was spun at 11 000g, for 20 min at 4°C and

the supernatant (S10) stored at -70°C . The extract concentration was $>25 A_{260}$ U/ml. S200 and P200 (Ribo) were prepared as described (19). The $50\ \mu\text{l}$ *in vitro* translation mixture contained $25\ \mu\text{l}$ S10 extract, $5\ \mu\text{l}$ $10\times$ translation mix ($125\ \text{mM}$ HEPES pH 7.3, $10\ \text{mM}$ ATP, $2\ \text{mM}$ GTP, $2\ \text{mM}$ CTP, $2\ \text{mM}$ UTP, $100\ \text{mM}$ creatine phosphate, $0.2\ \text{mM}$ amino acids, $1\ \text{mg/ml}$ creatine phosphokinase), $5\ \mu\text{l}$ salt mix ($1\ \text{M}$ potassium acetate, $30\ \text{mM}$ MgCl_2 , $2.5\ \text{mM}$ spermidine), $1\ \mu\text{l}$ methionine ($1\ \text{mM}$), $40\ \text{U}$ RNase inhibitor and $1\ \mu\text{g}$ luciferase-encoding RNA. When the effect of PABP and its truncated versions was tested, PABP, NTD and CTD in native and heat-denatured form were added at the indicated amounts, before the mixtures (prepared in at least duplicate) were incubated at 30°C . Aliquots in duplicate were taken at 90 min, and luciferase activity was tested with the Luciferase Assay System (Promega) in the luminometer Lucy-3 of Anthos, Germany. Luciferase activity is expressed in relative light units (RLU).

RESULTS AND DISCUSSION

eIF4G is not cleaved by HAV 3C^{pro}

To evade the cells' antiviral machinery early on in the viral life cycle, proteinases of some picornaviruses cleave eIF4G that serves as scaffolding protein in the cap-binding complex eIF4F (13,15). Whereas host translation is subsequently blocked, viral IRES-mediated translation proceeds and is even stimulated in the presence of cleaved eIF4G (14). HAV replicates in a highly protracted and asynchronous fashion in cells. This particular replication feature, combined with low yields of viral progeny, was often posed as argument that specific viral effects on the host metabolism could not be identified in HAV-infected cells. To provide direct evidence for the unconfirmed observation that eIF4G remained intact in HAV-infected cells (14), eIF4G cleavage by the one and only HAV proteinase 3C^{pro} *in vitro* was directly assessed. To this aim, endogenous eIF4G of a S10 cell extract was subjected to treatment with purified viral proteinases. After incubation with HAV 3C^{pro} for 6 h at 37°C , no cleavage products were detectable in the anti-eIF4G blot (Figure 1A, lower panel, compare lanes 1 and 2). However, and in accordance with previously reported data (16), eIF4G was almost completely cleaved by CVB3 3C^{pro} (lane 3) under the same conditions. Moreover, numerous attempts to demonstrate eIF4G cleavage *in vivo* were unsuccessful. In no case, eIF4G cleavage products were detectable. These approaches included eIF4G analysis in HAV-infected cells and after vaccinia virus-mediated over-expression of HAV 3C^{pro} and its proteolytically active precursor 3ABC. eIF4G was cleaved by CVB3 3C^{pro} that was used as control, but not by HAV 3C^{pro} (Figure 1S, in Supplementary Data). The resistance of eIF4G to HAV 3C^{pro} and its precursor-mediated cleavage clearly is in line with the requirement of intact eIF4G for translation initiation by the HAV IRES (33,55). As eIF4G cleavage correlates with enteroviral cytopathology, lack of HAV 3C^{pro}-mediated eIF4G cleavage is also consistent with the noncytolytic replication of HAV. Strikingly,

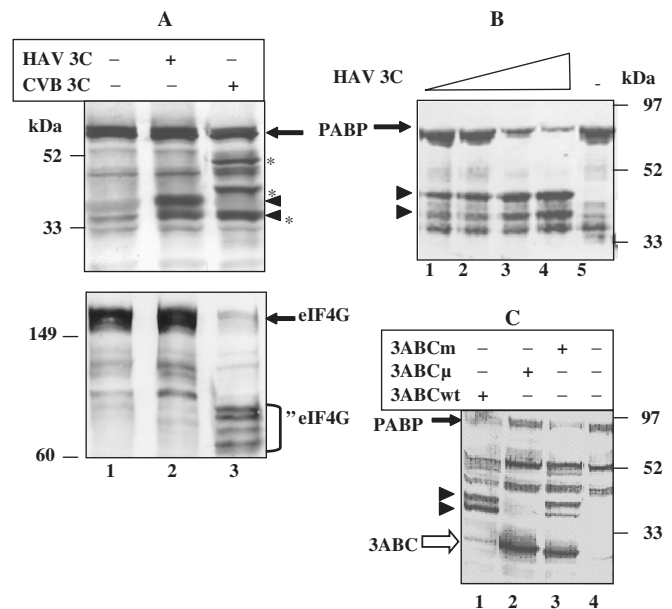


Figure 1. HAV 3C^{pro} cleaves PABP, but not eIF4G (A). The S10 extract of Huh-7 cells was incubated for 6 h at 37°C with HAV 3C^{pro} and CVB3 3C^{pro} *in vitro* and eIF4G and PABP cleavage was analyzed by immunoblot using anti-eIF4G (lower panel) or anti-PABP (upper panel), respectively. Anti-PABP was raised against a synthetic peptide sequence in the RRM4 of human PABP (63). Lane 1—no proteinase added, lanes 2 and 3—the proteinases marked were added to a final concentration of $1.4\ \mu\text{M}$. Products of PABP cleavage by HAV 3C are marked with arrowheads, products of CVB3 3C with asterisks. ΔeIF4G indicates various cleavage products. (B) Concentration dependence of HAV 3C cleavage *in vitro* of purified recombinant His-tagged PABP ($400\ \text{ng}$). In lanes 1–4, the concentration of HAV 3C was 1, 2, 5 and $10\ \mu\text{M}$, respectively. Anti-His was used to identify complete PABP and its N-terminal cleavage products. (C) *In vivo* cleavage of recombinant His-tagged PABP by HAV 3C precursors, both expressed in Huh-7 cells with the help of vaccinia virus vTF7-3. As described in the text, proteolytically active 3ABCwt carries the wild-type sequence and 3ABCmut contains non-cleavable 3A/3B and 3B/3C junctions; proteolytically inactive 3ABC μ is mutated in the active site of 3C^{pro} (C172A). The cleavage products were detected by anti-His. Note that the N-terminally His-tagged 3C precursors were also detected (empty arrow).

HAV IRES-dependent translation does not only require complete eIF4G, but the entire eIF4F complex. This was clearly evidenced by the finding that 4E-binding protein interfered with HAV IRES activity, supposedly by sequestering eIF4E and preventing its interaction with eIF4G (33). Moreover, addition of cap-analog blocked the HAV IRES activity *in vitro*, indicating that translation initiation by the HAV IRES requires association of eIF4E with eIF4G and an empty cap-binding pocket of eIF4E (55,56). Combined with earlier observations, all evidence points to the notion that translation initiation by the HAV IRES requires essentially the same translation factors as capped host mRNAs and seems to compete with those (2,27,55,56). This notion presents a surprising paradox that the function of the 3' part of the HAV 5'NTR in translation is currently indistinguishable from cap-dependent translation, although it folds into the conformation of a genuine IRES and mediates the expression of a second cistron in a bicistronic construct (33).

Apparently, HAV cap-independent translation does not benefit from the advantage that is usually supplied by viral or cellular IRES.

HAV 3C^{pro} cleaves PABP

PABP is a translation initiation factor that together with eIF4G forms a bridge between the 3' and 5' ends of mRNA, including picornaviral RNA (2,3,5,8). The interaction between eIF4G and PABP is sufficient for mRNA circularization (6). PABP cleavage has been implicated in the cytopathic and apoptotic degeneration of infected and non-infected cells (5,17). To investigate whether PABP is a direct substrate of HAV 3C^{pro}, the same cleavage reaction used to identify eIF4G cleavage products was analyzed by immunoblot with anti-PABP (Figure 1A, upper panel). Consistent with previously published data (17,18), CVB3 3C^{pro} partially cleaved PABP, resulting in three products (lane 3, marked with asterisks). PABP cleavage by HAV 3C^{pro} generated two products (lane 2, marked with arrowheads). The smallest HAV 3C cleavage product migrated with the same mobility as the smallest cleavage product of CVB3 3C^{pro}, suggesting that HAV 3C^{pro} also cleaves near or at the dipeptide sequence (Q/T) of PABP at position 415/416, which was proposed as site of cleavage by enteroviral 3C^{pro} (18). Cleavage at this site separates two essential functions of PABP: the NTD with four RRM's binds RNA, whereas the CTD interacts with various translation factors (5,7,9,10).

For poliovirus, it was demonstrated that initiation factor- and ribosome-associated PABP was specifically targeted by the viral proteinase *in vitro*, whereas non-ribosome-associated PABP was mostly resistant to 3C cleavage (18). However, no difference in PABP cleavability by HAV 3C^{pro} was detectable when the S200 and P200 (Ribo) fractions of Huh-7 cell extracts were incubated with purified recombinant HAV 3C^{pro} (Supplementary Figure 2S). Moreover, under no condition PABP cleavage *in vivo* was complete when CVB3 or HAV 3C^{pro} was used, suggesting that compartmentalization or an alternative conformation (PABP complexed with proteins or RNA) may modulate PABP cleavage.

Notwithstanding, PABP cleavage by HAV 3C^{pro} was further analyzed to ensure that PABP was a direct substrate of HAV 3C^{pro}. For this, purified recombinant PABP with an N-terminal His-tag was incubated for various times (data not shown) or with increasing concentrations of HAV 3C. In addition to anti-PABP (data not shown), anti-His was used in the immunoblot, in order to specifically demonstrate the N-terminal nature of the cleavage products. As depicted in Figure 1B, purified PABP with an N-terminal His-tag was almost completely cleaved when HAV 3C^{pro} was used up to a 10 μ M concentration (lanes 1–4). Again, two N-terminally tagged cleavage products were detectable by anti-His (marked by arrowheads). The cleavage products that were derived from native and recombinant PABP and recognized either by anti-PABP and/or anti-His were indistinguishable (Figure 1A and B, respectively), implying that they were C-terminally truncated.

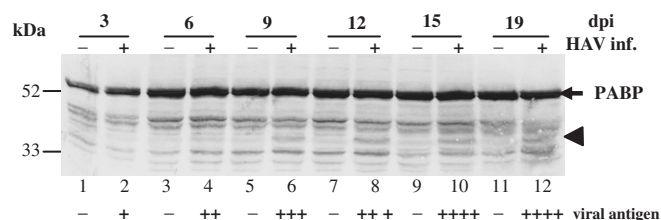


Figure 2. PABP cleavage in HAV-infected Huh-7 cells. Clarified lysates of mock (lanes with odd numbers) and HAV-infected cells (lanes with even numbers) obtained at the indicated days post-infection (dpi) were separated by SDS-PAGE, transferred onto nitrocellulose membranes and probed with anti-PABP. Viral antigen in the same extracts was determined by ELISA and is presented below the lanes (+, antigenicity 3-fold; ++, 9-fold; +++, 20-fold; +++++ more than 30-fold over negative (-) controls).

In HAV-infected cells, 3C^{pro} co-exists with the precursor polypeptide 3ABC that also shows proteolytic activity with slightly different substrate specificity (38,52). To test whether this form of the viral proteinase was active and yielded different PABP cleavage products, proteolytically active 3ABCwt and 3ABCm, with non-cleavable 3A/3B and 3B/3C junctions, were co-expressed with His-tagged PABP and with the help of vaccinia virus vTF7-3. Proteolytically inactive 3ABC μ , which carries a mutation at the active site of 3C^{pro} (C172A), was used as a control. The expression and cleavage products were detected by immunoblot with anti-His (Figure 1C). As expected, 3ABC μ did not cleave PABP (lane 2). Both active proteinases, 3ABCwt (lane 1) and 3ABCm (lane 3), generated two PABP cleavage products *in vivo* (arrowheads) that corresponded to those produced by *in vitro* cleavage with the purified mature enzyme (Figure 1A and B). The proteinase precursors with an N-terminal His-tag were also detected in the blot (empty arrow). Due to its autoproteolytic activity resulting in 3BC and 3C, lower amounts of unprocessed 3ABCwt (lane 1) were found, as compared to either 3ABC μ (lane 2) or 3ABCm (lane 3). The data suggest that mature proteinase 3C^{pro} and its precursor 3ABC have the same PABP cleavage specificity.

In order to evaluate the extent of PABP cleavage in HAV-infected cells, cell extracts of infected and non-infected Huh-7 cells were analyzed by immunoblot with anti-PABP (Figure 2). To correlate viral replication with the extent of PABP cleavage, cell morphology was judged by light microscopy and HAV particle formation was determined in the same experiment. Compared to uninfected cells, no morphological changes were observed at any time during viral replication, underlining the non-cytopathogenic replication of HAV in this hepatoma cell line (data not shown). Under the chosen infection conditions, the small PABP cleavage product of 41 kDa (arrowhead) was detectable starting 9 days post-infection (lane 6) when viral replication was actively proceeding. The cleavage product detected in infected cells comigrated with the polypeptide generated by PABP cleavage *in vitro* with purified HAV 3C^{pro} and with the small cleavage product of CVB3 3C^{pro} (data not shown). Interestingly, only the small PABP cleavage product was detected in

HAV-infected cells as compared to *in vivo* or *in vitro* cleavage with recombinant 3C^{pro} (Figure 1). Although viral particle accumulation still continued until the end of the experiment (indicated below the lanes), the relative small amount of the 41 kDa PABP cleavage product remained constant. Independent of the infectious dose used, the extent of PABP cleavage was always low and only detectable by the appearance of the cleavage product. The highly limited PABP cleavage is in accordance with the noncytolytic replication of HAV that does not shut off host protein synthesis. Based on results shown below, we speculate that HAV 3C^{pro} targets only those PABP molecules that are bound to the viral poly(A) tail and associated with the translation complex. It is expected that the majority of PABP molecules, in particular those involved in host protein translation, remains intact due to inaccessibility to HAV 3C. It is also possible that the low concentration or short half-life of 3C^{pro} *in vivo* is the reason for the incomplete cleavage (57). Collectively, the *in vitro* and *in vivo* cleavage data clearly show that PABP is a direct substrate of HAV 3C^{pro}. Based on its electrophoretic mobility and compared with the PABP products generated by enteroviral 3C cleavage, it can be concluded that HAV 3C^{pro} removes the C-terminal third of PABP that mediates PABP oligomerization and recruits proteins involved in translation initiation and termination (18). The exact locations of the HAV 3C cleavage sites within PABP await sequence analysis.

Functional role of C-terminally truncated PABP

Apparently PABP cleavage in HAV-infected cells is strictly limited to a particular portion of PABP molecules, suggesting that HAV 3C^{pro}-mediated cleavage might support a viral function rather than concern host translation. Possibly, HAV 3C^{pro} is only active on PABP molecules associated with the viral poly(A) tail. In fact, only a small portion of the viral genomes appears to be unpackaged and translationally active in HAV-infected cells (58). In the next experiments, we tested the recently proposed hypothesis that 3C^{pro} cleavage of PABP might be a precondition for viral translation arrest (5). Similar to studies described elsewhere, transcripts containing the firefly luciferase preceded by the HAV IRES were translated *in vitro* using either the reticulocyte lysate (data not shown) or S10 extract that were pretreated with HAV 3C^{pro} (27). As under the experimental conditions used, not only PABP, but also PCBP and PTB were found to be cleaved, the effect of cleaved PABP on HAV translation could not be singled out under this experimental condition (data not shown). To evade the unintended cleavage of host proteins, we next tested the effect of purified NTD added to *in vitro* translation reactions primed with synthetic transcripts representing the HAV and PV replicon. The S10 extract of Huh-7 cells was supplemented with purified PABP, NTD and CTD and IRES translation was monitored by the reporter gene activity. Cap-independent translation of the HAV replicon was mostly unaffected by the addition of intact PABP or CTD (Figure 3A, bars 3 and 4), but inhibited when NTD was present (bar 2). In the assays,

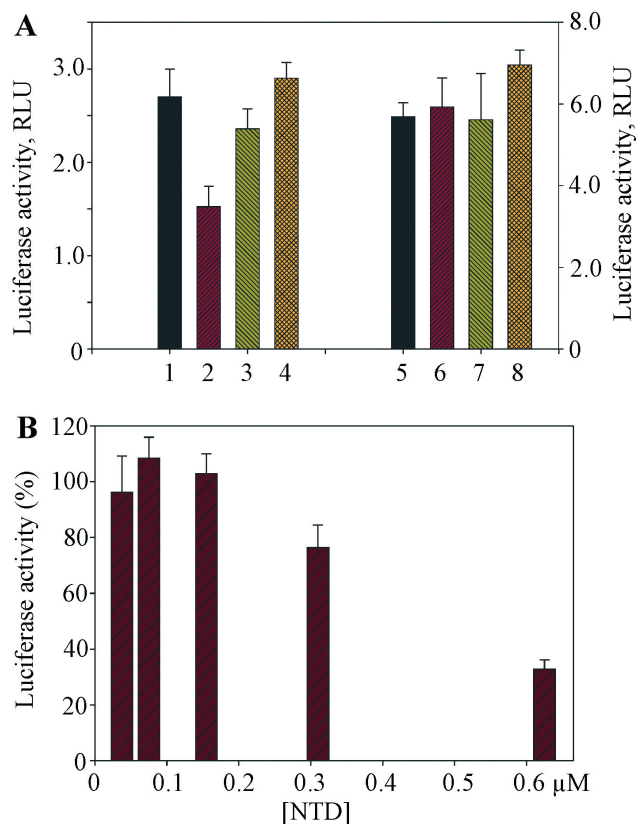


Figure 3. Effect of PABP and its NTD and CTD on HAV and PV IRES translation. (A) *In vitro* expression of the HAV (bars 1–4 and left ordinate) and PV replicon RNA (bars 5–8 and right ordinate). The translation of the luciferase reporter gene was analyzed in S10 extracts supplemented with PABP (bars 1 and 5), NTD (bars 2 and 6), CTD (bars 3 and 7) or buffer (bars 4 and 8). (B) *In vitro* expression of RNA HAV-IRES-Luc in S10 extracts supplemented with increasing concentrations of native and heat-denatured NTD. Luciferase activity (RLU) in the presence of native NTD was normalized to the activity determined in the presence of denatured protein.

the NTD and CTD concentration was 0.3 μM and thus in the range of endogenous PABP (9). Under the same conditions, translation of the PV replicon RLuc31 was two times higher (right ordinate) and no suppression was observed (Figure 3A, lanes 5–8). The inhibitory effect of NTD on HAV IRES translation was also detectable when a synthetic transcript derived from pHAV-IRES-luc and containing the firefly luciferase preceded by the HAV IRES was expressed in the S10 extract (Figure 3B). In this experiment, the effect of native NTD was normalized by that of the heat-denatured protein set at 100%. Under these experimental conditions, NTD at concentrations equal to and higher than 0.3 μM specifically suppressed the function of the HAV IRES. No effect was observed when CTD was added to the system (data not shown). These findings clearly demonstrate that the N-terminal domain of PABP has a dominant negative effect on HAV IRES-mediated translation. They suggest that NTD might either change the conformation of the HAV IRES or of eIF4G or compete with eIF4G for binding to the IRES.

Interaction of complete and truncated PABP with terminal RNA elements

HAV IRES-dependent translation competes with and precludes subsequent negative strand RNA synthesis on the same RNA molecule. For PV, several viral and host proteins in association with viral 5' terminal RNA structures were proposed to be involved in RNA template switching from translation to replication (5,34,59–61). In particular, cleavage of RNA-binding host proteins (PABP, PCBP, PTB, La autoantigen) might be implicated in this regulatory step (5,60,61). In line with this concept, we were interested to search for a positive role of NTD in HAV RNA synthesis. So far, no *in vitro* system is available to directly study HAV genome replication. As binding to terminal RNA structures of the viral genome is an essential prerequisite for the role of a host or viral protein and therefore a surrogate feature for RNA synthesis, we compared the binding specificities and affinities of PABP and NTD to terminal RNA elements of the HAV genome. In this context, it is also interesting to note that biosynthesis of PABP is inhibited by autoregulatory binding of PABP to the 5'NTR of its own mRNA (62).

The functionality and specificity of complete and truncated recombinant PABP was first determined by their interaction with the HAV 3' NTR, using EMSAs. The apparent equilibrium-binding constant (app. K_{eq}) was determined in additional titration experiments (data not shown). No binding of recombinant PABP to the HAV 3' NTR lacking the poly(A) tail was observed (Figure 4A, lanes 1–4, app. $K_{eq} \gg 10 \mu\text{M}$). Ribonucleoprotein (RNP) complex formation was seen when the RNA ligand contained a poly(A) tail of 14 (data not shown) or 20 residues (lanes 5–9, app. $K_{eq} = 0.05 \mu\text{M}$). PABP binding to the 3'NTR was even more enhanced when the poly(A) tail comprised 60 residues (lanes 10–13, app. $K_{eq} < 0.05 \mu\text{M}$). This app. K_{eq} was similar to what has been reported for the 3'NTR of PV with a poly(A) tail of 80 nt (60). As expected, binding of multiple copies of PABP to the poly(A) tail was noticeable by the formation of RNPs with different mobilities. The NTD of PABP also interacted with the polyadenylated HAV 3'NTR, yet somewhat less efficiently (data not shown). Our results confirm the notion that cooperative PABP binding to the HAV 3'NTR is dependent on the poly(A) tail length and that binding requires the N-terminal RRM of PABP.

Surprisingly, initiation of enteroviral negative strand RNA synthesis is regulated by *cis*-acting RNA elements present at the distant 5' end of the positive strand RNA genome (34,42,59). Moreover, a protein bridge formed by PCBP and PABP was proposed to be required for PV negative strand synthesis (60). In line with such a model, we were interested to test the possibility that C-terminally truncated PABP might be directly involved in a replication function mapping to the HAV 5'NTR. Both RNA structural elements comprising bases 1–94 and 95–148 (pY1) were previously found to be essential for HAV RNA synthesis (26) and were therefore tested for their direct interaction with PABP and NTD. Whereas RNA1–94 did not directly bind to either complete or

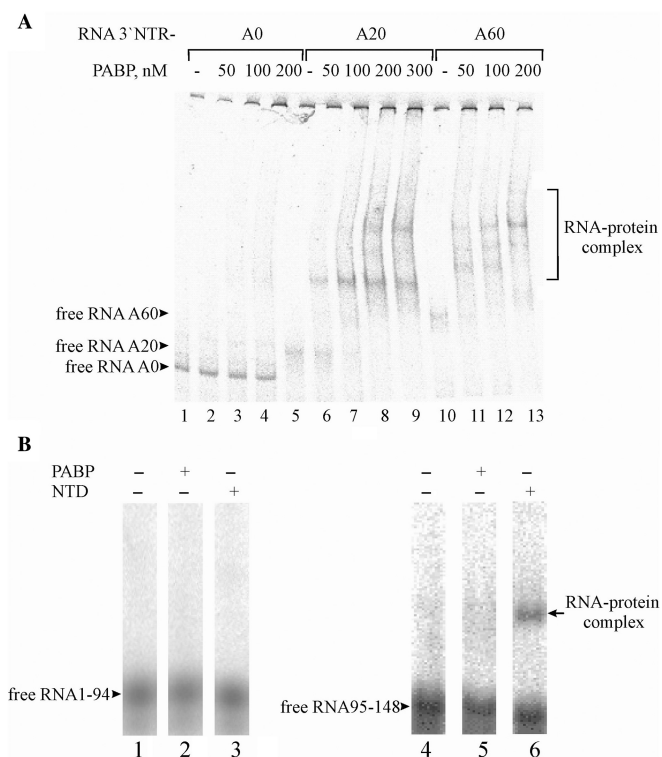


Figure 4. Interaction of PABP and NTD with RNA structures at the 3' and 5' end of the HAV genome. (A) PABP interaction with the HAV 3'NTR without or with a poly(A) tail of different lengths (A20 and A60 as indicated above the lanes). Purified PABP was incubated in increasing concentrations (indicated above the lanes) with radiolabeled RNA and RNP complex formation was analyzed by EMSA on a native polyacrylamide gel. (B) Differential-binding capacity of PABP and NTD. Complex formation of PABP and NTD (both $0.7 \mu\text{M}$) with RNA1-94 (lanes 1–3) and pY1 (RNA95–148) (lanes 4–6) was assessed by EMSA. Mobility of the free RNAs is marked on the left; the RNA–protein complexes are marked on the right.

C-terminally truncated PABP (Figure 4B, lanes 1–3), incubation of purified NTD with radiolabeled pY1 yielded a RNP that was discernable by EMSA (lanes 4–6). In contrast to PABP (lane 5), NTD at the same concentration ($0.7 \mu\text{M}$) was able to shift the mobility of pY1 (lane 6). Based on the relative app. K_{eq} that was calculated for PABP and NTD, it was concluded that NTD was ~ 10 times more efficient in binding pY1 (see Supplementary Figure 3S). The data indicate that removal of the CTD from PABP-enhanced binding to pY1 in the HAV 5'NTR, a structure pivotal in virus replication. Although speculative, the data provide the basis for the hypothesis that PABP cleavage mediated by HAV 3C^{pro} might be involved in HAV template switching from translation to genome replication.

In summary, we report that HAV 3C^{pro} cleaves PABP, which was shown to mediate the synergistic effect of the poly(A) tail on IRES-dependent translation and substantially enhance protein synthesis (1–3). We also show that the N-terminal fragment of PABP inhibits HAV IRES-dependent translation (Figure 3) and has an enhanced binding capacity to pY1 (Figures 4 and 3S). Based on these new findings and a model proposed for poliovirus

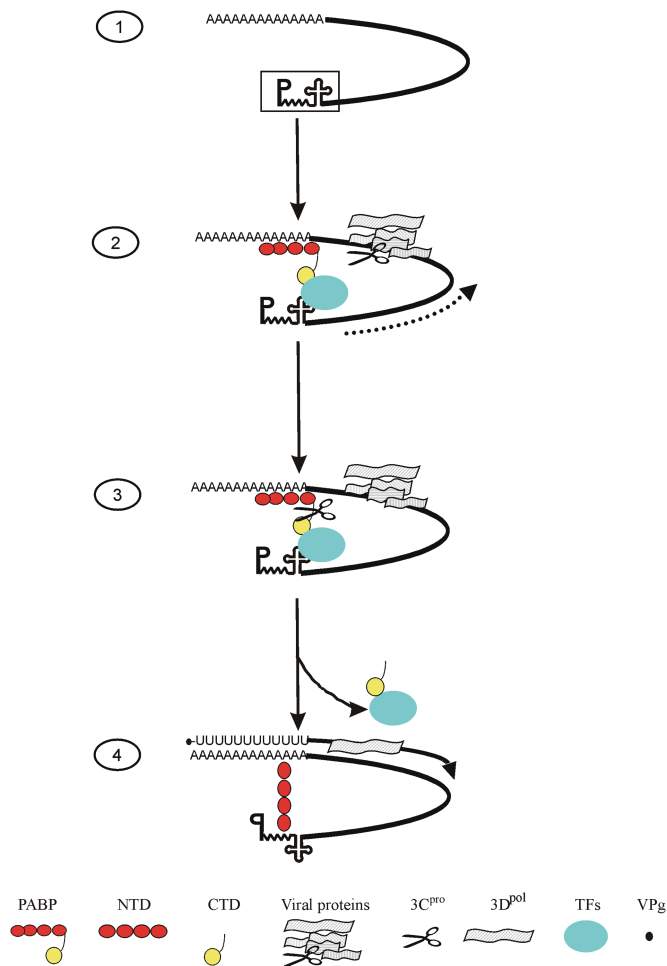


Figure 5. Putative model for the role of PABP cleavage in HAV template switching from protein to RNA synthesis. (1) HAV RNA and secondary structural elements within the 5'NTR (boxed area: 5' terminal domain I, 'P'; pY1, 'zigzag' and IRES, 'cloverleaf-like structure'). VPg covalently linked to the 5' end is not shown. (2) For enhanced translation initiation, a protein bridge is formed by PABP and translation factors (TFs, see symbol explanation at the bottom), thereby circularizing the viral RNA. Translation proceeds in the 5' to 3' direction (dotted arrow). Products of translation and proteolytic processing are the viral polyprotein, intermediate and mature proteins, including proteinase 3C^{pro} (scissor) and polymerase 3D^{pol}. (3) HAV 3C^{pro} specifically cleaves PABP bound to the viral poly(A) and engaged in IRES translation. (4) The cleavage product NTD remains bound to the poly(A) tail. It no longer interacts with the various eIFs and therefore precludes ribosome binding to the IRES. The interaction of eIF4G to RRM2 is not depicted. Possibly, released CTD sequesters some translation factors, thus preventing ribosome recycling (64). Through its enhanced interaction with pY1, NTD might bridge the RNA ends, thereby favoring the synthesis of negative strand RNA by the replication complex (solid arrow, for simplicity only polymerase 3D^{pol} is shown) late in the infectious cycle. The simultaneous interaction of NTD with poly(A) and pY1 was not tested. Altered (mirrored) symbols for RNA structures in the 5'NTR point to possible alternative conformations. Additional cellular proteins possibly involved in the regulation of template switching (e.g. PCBP, PTB, La autoantigen) are not depicted.

(60), we suggest a model to explain the putative role of PABP cleavage in HAV RNA template switching (Figure 5). In contrast to poliovirus that shuts off host translation by cleaving eIF4G, HAV translation

constantly competes with host translation for initiation factors (e.g. eIF4G) and is therefore highly inefficient (1,36,37). After adequate amounts of translation and polyprotein processing products have accumulated, PABP bound to the HAV poly(A) tail is specifically targeted by HAV 3C^{pro}. In contrast to the complete protein, the resulting poly(A) bound N-terminal cleavage product of PABP (NTD) no longer bridges the poly(A) tail to the IRES, but rather to the 5'RNA structure pY1, which was shown to be essential for viral replication (26). As a consequence, ribosomes cease to recycle in order to initiate HAV IRES translation. Subsequently, stalled protein synthesis gives way to viral RNA synthesis that uses the same RNA template as translation, yet in the opposite direction. To better understand the exact molecular mechanisms, in particular the possible involvement of other viral and/or cellular components, further studies are needed. Not depicted in our model is the possibility that truncated PABP sequesters and/or modifies the functional conformation eIF4G, such that ribosome re-initiation at the 5'IRES structure is no longer possible. As—to our current knowledge—the major components needed for HAV IRES-dependent translation are the same as for cap-dependent host translation (56), it is likely that the model proposed for cellular translation arrest (5) holds also true for HAV translation and provides an example for the delicate viral–host interplay to the best of both partners.

SUPPLEMENTARY DATA

Supplementary Data are available at NAR Online.

ACKNOWLEDGEMENTS

We thank Dr A. Andino, Dr M. Görlach, Dr G.J. Goodall, Dr M. Hentze, Dr M. Kiledjian, Dr R. Lloyd, Dr B. Moss, Dr R.E. Rhoads and Dr R. Zell for material used in this study. The help of Ms S. Cordes, M. Bohm, B. Andresen and K. Thiele-Bössel is highly appreciated. We are grateful to P.K. Müller for reading the manuscript. Work in the laboratory is funded by the Deutsche Forschungsgemeinschaft (DFG, projects Pe494/4 and Ga304/7-1). Funding to pay the Open Access publication charges for this article was provided by the DFG.

Conflict of interest statement. None declared.

REFERENCES

- Michel, Y.M., Poncet, D., Piron, M., Kean, K.M. and Borman, A.M. (2000) Cap-Poly(A) synergy in mammalian cell-free extracts. Investigation of the requirements for poly(A)-mediated stimulation of translation initiation. *J. Biol. Chem.*, **275**, 32268–32276.
- Michel, Y.M., Borman, A.M., Paulous, S. and Kean, K.M. (2001) Eukaryotic initiation factor 4G-poly(A) binding protein interaction is required for poly(A) tail-mediated stimulation of picornavirus internal ribosome entry segment-driven translation but not for X-mediated stimulation of hepatitis C virus translation. *Mol. Cell. Biol.*, **21**, 4097–4109.
- Bergamini, G., Preiss, T. and Hentze, M.W. (2000) Picornavirus IRESes and the poly(A) tail jointly promote cap-independent translation in a mammalian cell-free system. *RNA*, **6**, 1781–1790.

4. Svitkin, Y.V., Imataka, H., Khaleghpour, K., Kahvejian, A., Liebig, H.D. and Sonenberg, N. (2001) Poly(A)-binding protein interaction with eIF4G stimulates picornavirus IRES-dependent translation. *RNA*, **7**, 1743–1752.
5. Lloyd, R.E. (2006) Translational control by viral proteinases. *Virus Res.*, **119**, 76–88.
6. Wells, S.E., Hillner, P.E., Vale, R.D. and Sachs, A.B. (1998) Circularization of mRNA by eukaryotic translation initiation factors. *Mol. Cell.*, **2**, 135–140.
7. Kuhn, U. and Wahle, E. (2004) Structure and function of poly(A) binding proteins. *Biochim. Biophys. Acta.*, **1678**, 67–84.
8. Kahvejian, A., Svitkin, Y.V., Sukarieh, R., M'Boutchou, M.N. and Sonenberg, N. (2005) Mammalian poly(A)-binding protein is a eukaryotic translation initiation factor, which acts via multiple mechanisms. *Genes Dev.*, **19**, 104–113.
9. Gorlach, M., Burd, C.G. and Dreyfuss, G. (1994) The mRNA poly(A)-binding protein: localization, abundance, and RNA-binding specificity. *Exp. Cell. Res.*, **211**, 400–407.
10. Mullin, C., Duning, K., Barnekow, A., Richter, D., Kremerskothen, J. and Mohr, E. (2004) Interaction of rat poly(A)-binding protein with poly(A)- and non-poly(A) sequences is preferentially mediated by RNA recognition motifs 3+4. *FEBS Lett.*, **576**, 437–441.
11. Mangus, D.A., Evans, M.C. and Jacobson, A. (2003) Poly(A)-binding proteins: multifunctional scaffolds for the post-transcriptional control of gene expression. *Genome Biol.*, **4**, 223.
12. Khanna, R. and Kiledjian, M. (2004) Poly(A)-binding-protein-mediated regulation of hDcp2 decapping in vitro. *EMBO J.*, **23**, 1968–1976.
13. Liebig, H.D., Ziegler, E., Yan, R., Hartmuth, K., Klump, H., Kowalski, H., Blaas, D., Sommergruber, W., Frasel, L. et al. (1993) Purification of two picornaviral 2A proteinases: interaction with eIF-4 gamma and influence on in vitro translation. *Biochemistry*, **32**, 7581–7588.
14. Ziegler, E., Borman, A.M., Deliat, F.G., Liebig, H.D., Jugovic, D., Kean, K.M., Skern, T. and Kuechler, E. (1995) Picornavirus 2A proteinase-mediated stimulation of internal initiation of translation is dependent on enzymatic activity and the cleavage products of cellular proteins. *Virology*, **213**, 549–557.
15. Borman, A.M., Kirchweger, R., Ziegler, E., Rhoads, R.E., Skern, T. and Kean, K.M. (1997) eIF4G and its proteolytic cleavage products: effect on initiation of protein synthesis from capped, uncapped, and IRES-containing mRNAs. *RNA*, **3**, 186–196.
16. Joachims, M., Van Breugel, P.C. and Lloyd, R.E. (1999) Cleavage of poly(A)-binding protein by enterovirus proteases concurrent with inhibition of translation in vitro. *J. Virol.*, **73**, 718–727.
17. Kerekatte, V., Keiper, B.D., Badoff, C., Cai, A., Knowlton, K.U. and Rhoads, R.E. (1999) Cleavage of Poly(A)-binding protein by coxsackievirus 2A protease in vitro and in vivo: another mechanism for host protein synthesis shutoff? *J. Virol.*, **73**, 709–717.
18. Kuyumcu-Martinez, N.M., Joachims, M. and Lloyd, R.E. (2002) Efficient cleavage of ribosome-associated poly(A)-binding protein by enterovirus 3C protease. *J. Virol.*, **76**, 2062–2074.
19. Kuyumcu-Martinez, N.M., Van Eden, M.E., Younan, P. and Lloyd, R.E. (2004) Cleavage of poly(A)-binding protein by poliovirus 3C protease inhibits host cell translation: a novel mechanism for host translation shutoff. *Mol. Cell. Biol.*, **24**, 1779–1790.
20. Brown, E.A., Day, S.P., Jansen, R.W. and Lemon, S.M. (1991) The 5' nontranslated region of hepatitis A virus RNA: secondary structure and elements required for translation in vitro. *J. Virol.*, **65**, 5828–5838.
21. Brown, E.A., Zajac, A.J. and Lemon, S.M. (1994) In vitro characterization of an internal ribosomal entry site (IRES) present within the 5' nontranslated region of hepatitis A virus RNA: comparison with the IRES of encephalomyocarditis virus. *J. Virol.*, **68**, 1066–1074.
22. Glass, M.J., Jia, X.Y. and Summers, D.F. (1993) Identification of the hepatitis A virus internal ribosome entry site: in vivo and in vitro analysis of bicistronic RNAs containing the HAV 5' noncoding region. *Virology*, **193**, 842–852.
23. Le, S.Y., Chen, J.H., Sonenberg, N. and Maizel, J.V. Jr (1993) Conserved tertiary structural elements in the 5' nontranslated region of cardiomyovirus, aphthovirus and hepatitis A virus RNAs. *Nucleic Acids Res.*, **21**, 2445–2451.
24. Schultz, D.E., Honda, M., Whetter, L.E., McKnight, K.L. and Lemon, S.M. (1996) Mutations within the 5' nontranslated RNA of cell culture-adapted hepatitis A virus which enhance cap-independent translation in cultured African green monkey kidney cells. *J. Virol.*, **70**, 1041–1049.
25. Whetter, L.E., Day, S.P., Elroy-Stein, O., Brown, E.A. and Lemon, S.M. (1994) Low efficiency of the 5' nontranslated region of hepatitis A virus RNA in directing cap-independent translation in permissive monkey kidney cells. *J. Virol.*, **68**, 5253–5263.
26. Shaffer, D.R., Brown, E.A. and Lemon, S.M. (1994) Large deletion mutations involving the first pyrimidine-rich tract of the 5' nontranslated RNA of human hepatitis A virus define two adjacent domains associated with distinct replication phenotypes. *J. Virol.*, **68**, 5568–5578.
27. Borman, A.M., Michel, Y.M. and Kean, K.M. (2001) Detailed analysis of the requirements of hepatitis A virus internal ribosome entry segment for the eukaryotic initiation factor complex eIF4F. *J. Virol.*, **75**, 7864–7871.
28. Paulous, S., Malnou, C.E., Michel, Y.M., Kean, K.M. and Borman, A.M. (2003) Comparison of the capacity of different viral internal ribosome entry segments to direct translation initiation in poly(A)-dependent reticulocyte lysates. *Nucleic Acids Res.*, **31**, 722–733.
29. Graff, J., Cha, J., Blyn, L.B. and Ehrenfeld, E. (1998) Interaction of poly(rC) binding protein 2 with the 5' noncoding region of hepatitis A virus RNA and its effects on translation. *J. Virol.*, **72**, 9668–9675.
30. Schultz, D.E., Hardin, C.C. and Lemon, S.M. (1996) Specific interaction of glyceraldehyde 3-phosphate dehydrogenase with the 5'-nontranslated RNA of hepatitis A virus. *J. Biol. Chem.*, **271**, 14134–14142.
31. Yi, M., Schultz, D.E. and Lemon, S.M. (2000) Functional significance of the interaction of hepatitis A virus RNA with glyceraldehyde 3-phosphate dehydrogenase (GAPDH): opposing effects of GAPDH and polypyrimidine tract binding protein on internal ribosome entry site function. *J. Virol.*, **74**, 6459–6468.
32. Gosert, R., Chang, K.H., Rijnbrand, R., Yi, M., Sangar, D.V. and Lemon, S.M. (2000) Transient expression of cellular polypyrimidine-tract binding protein stimulates cap-independent translation directed by both picornaviral and flaviviral internal ribosome entry sites in vivo. *Mol. Cell. Biol.*, **20**, 1583–1595.
33. Borman, A.M. and Kean, K.M. (1997) Intact eukaryotic initiation factor 4G is required for hepatitis A virus internal initiation of translation. *Virology*, **237**, 129–136.
34. Barton, D.J., Morasco, B.J. and Flanagan, J.B. (1999) Translating ribosomes inhibit poliovirus negative-strand RNA synthesis. *J. Virol.*, **73**, 10104–10112.
35. Brack, K., Berk, I., Magulski, T., Lederer, J., Dotzauer, A. and Vallbracht, A. (2002) Hepatitis A virus inhibits cellular antiviral defense mechanisms induced by double-stranded RNA. *J. Virol.*, **76**, 11920–11930.
36. Gauss-Muller, V. and Deinhardt, F. (1984) Effect of hepatitis A virus infection on cell metabolism in vitro. *Proc. Soc. Exp. Biol. Med.*, **175**, 10–15.
37. Kean, K.M. (2003) The role of mRNA 5'-noncoding and 3'-end sequences on 40S ribosomal subunit recruitment, and how RNA viruses successfully compete with cellular mRNAs to ensure their own protein synthesis. *Biol. Cell*, **95**, 129–139.
38. Kusov, Y. and Gauss-Muller, V. (1999) Improving proteolytic cleavage at the 3A/3B site of the hepatitis A virus polyprotein impairs processing and particle formation, and the impairment can be complemented in trans by 3AB and 3ABC. *J. Virol.*, **73**, 9867–9878.
39. Sladic, R.T., Lagnado, C.A., Bagley, C.J. and Goodall, G.J. (2004) Human PABP binds AU-rich RNA via RNA-binding domains 3 and 4. *Eur. J. Biochem.*, **271**, 450–457.
40. Wang, Z., Day, N., Trifillis, P. and Kiledjian, M. (1999) An mRNA stability complex functions with poly(A)-binding protein to stabilize mRNA in vitro. *Mol. Cell. Biol.*, **19**, 4552–4560.
41. Gauss-Muller, V. and Kusov, Y.Y. (2002) Replication of a hepatitis A virus replicon detected by genetic recombination in vivo. *J. Gen. Virol.*, **83**, 2183–2192.
42. Andino, R., Rieckhof, G.E., Achacoso, P.L. and Baltimore, D. (1993) Poliovirus RNA synthesis utilizes an RNP complex formed around the 5'-end of viral RNA. *EMBO J.*, **12**, 3587–3598.
43. Kusov, Y., Gosert, R., Dzagurov, G., Shatirishvili, G., Gerhardt, M. and Gauss-Müller, V. (2004) Hepatitis A virus genome modified at

- its 3' terminus. In Columbus, F. (ed.), *Progress in Genome Research*, Nova Science Publishers Inc., NY, pp. 1–38.
44. Kusov, Y.Y. and Gauss-Muller, V. (1997) In vitro RNA binding of the hepatitis A virus proteinase 3C (HAV 3Cpro) to secondary structure elements within the 5' terminus of the HAV genome. *RNA*, **3**, 291–302.
 45. Martin, U., Jarasch, N., Nestler, M., Rassmann, A., Munder, T., Seitz, S., Zell, R., Wutzler, P. and Henke, A. (2007) Antiviral effects of pan-caspase inhibitors on the replication of coxsackievirus B3. *Apoptosis*, **12**, 525–533.
 46. Schultheiss, T., Sommergruber, W., Kusov, Y. and Gauss-Muller, V. (1995) Cleavage specificity of purified recombinant hepatitis A virus 3C proteinase on natural substrates. *J. Virol.*, **69**, 1727–1733.
 47. Kusov, Y.Y., Gosert, R. and Gauss-Muller, V. (2005) Replication and in vivo repair of the hepatitis A virus genome lacking the poly(A) tail. *J. Gen. Virol.*, **86**, 1363–1368.
 48. Kusov, Y.Y., Morace, G., Probst, C. and Gauss-Muller, V. (1997) Interaction of hepatitis A virus (HAV) precursor proteins 3AB and 3ABC with the 5' and 3' termini of the HAV RNA. *Virus Res.*, **51**, 151–157.
 49. Lane, D., Prentki, P. and Chandler, M. (1992) Use of gel retardation to analyze protein-nucleic acid interactions. *Microbiol. Rev.*, **56**, 509–528.
 50. Fuerst, T.R., Niles, E.G., Studier, F.W. and Moss, B. (1986) Eukaryotic transient-expression system based on recombinant vaccinia virus that synthesizes bacteriophage T7 RNA polymerase. *Proc. Natl Acad. Sci. USA*, **83**, 8122–8126.
 51. Yan, R., Rychlik, W., Etchison, D. and Rhoads, R.E. (1992) Amino acid sequence of the human protein synthesis initiation factor eIF-4 gamma. *J. Biol. Chem.*, **267**, 23226–23231.
 52. Probst, C., Jecht, M. and Gauss-Muller, V. (1998) Processing of proteinase precursors and their effect on hepatitis A virus particle formation. *J. Virol.*, **72**, 8013–8020.
 53. Beneduce, F., Kusov, Y., Klinger, M., Gauss-Muller, V. and Morace, G. (2002) Chimeric hepatitis A virus particles presenting a foreign epitope (HIV gp41) at their surface. *Antiviral Res.*, **55**, 369–377.
 54. Svitkin, Y.V. and Sonenberg, N. (2003) Cell-free synthesis of encephalomyocarditis virus. *J. Virol.*, **77**, 6551–6555.
 55. Ali, I.K., McKendrick, L., Morley, S.J. and Jackson, R.J. (2001) Activity of the hepatitis A virus IRES requires association between the cap-binding translation initiation factor (eIF4E) and eIF4G. *J. Virol.*, **75**, 7854–7863.
 56. Jackson, R.J. (2005) Alternative mechanisms of initiating translation of mammalian mRNAs. *Biochem. Soc. Trans.*, **33**, 1231–1241.
 57. Gladding, R.L., Haas, A.L., Gronros, D.L. and Lawson, T.G. (1997) Evaluation of the susceptibility of the 3C proteases of hepatitis A virus and poliovirus to degradation by the ubiquitin-mediated proteolytic system. *Biochem. Biophys. Res. Commun.*, **238**, 119–125.
 58. Anderson, D.A., Ross, B.C. and Locarnini, S.A. (1988) Restricted replication of hepatitis A virus in cell culture: encapsidation of viral RNA depletes the pool of RNA available for replication. *J. Virol.*, **62**, 4201–4206.
 59. Gamarnik, A.V. and Andino, R. (1998) Switch from translation to RNA replication in a positive-stranded RNA virus. *Genes Dev.*, **12**, 2293–2304.
 60. Herold, J. and Andino, R. (2001) Poliovirus RNA replication requires genome circularization through a protein-protein bridge. *Mol. Cell.*, **7**, 581–591.
 61. Back, S.H., Kim, Y.K., Kim, W.J., Cho, S., Oh, H.R., Kim, J.E. and Jang, S.K. (2002) Translation of polioviral mRNA is inhibited by cleavage of polypyrimidine tract-binding proteins executed by polioviral 3C(pro). *J. Virol.*, **76**, 2529–2542.
 62. Patel, G.P., Ma, S. and Bag, J. (2005) The autoregulatory translational control element of poly(A)-binding protein mRNA forms a heteromeric ribonucleoprotein complex. *Nucleic Acids Res.*, **33**, 7074–7089.
 63. Kuyumcu-Martinez, N.M., Belliot, G., Sosnovtsev, S.V., Chang, K.-O., Green, K.Y. and Lloyd, R.E. (2004) Calicivirus 3C-like proteinase inhibits cellular translation by cleavage of poly(A)-binding protein. *J. Virol.*, **78**, 8172–8182.
 64. Kozlov, G., Trempe, J.F., Khaleghpour, K., Kahvejian, A., Ekiel, I. and Gehring, K. (2001) Structure and function of the C-terminal PABC domain of human poly(A)-binding protein. *Proc. Natl Acad. Sci. USA*, **98**, 4409–4413.